STATISTICS, OPTIMIZATION AND INFORMATION COMPUTING
Stat., Optim. Inf. Comput., Vol. **15**, May 2026, pp 4464–4485.
Published online in International Academic Press (www.IAPress.org)

A New Flexible Transmuted Distribution: Theory and Application

H. M. Hamouda [1], and Khater A. E. Gad [2,*]

[1] *Department of Management Information System, College of Business and Economics, Qassim University, Buraidah, 52571, Qassim, Saudi Arabia, H.HAMOUDA@qu.edu.sa*
[2] *Faculty of Graduate Studies for Statistical Research, Cairo University, Egypt, khaterelrayany@gmail.com*

Abstract In this paper, we introduce a new three-parameter lifetime distribution, termed the Transmuted Ibrahim (TI) distribution, which is constructed by applying the quadratic rank transmutation map to the Ibrahim distribution. The TI distribution represents a novel three-parameter lifetime model arising from the quadratic rank transmutation of the Ibrahim distribution. In contrast to many existing transmuted families that emphasize purely formal generalization, the TI distribution is specifically designed to overcome concrete shortcomings of the original Ibrahim model, particularly its poor performance in representing high kurtosis and pronounced right-tail behavior while maintaining analytical and computational feasibility. The proposed framework addresses key weaknesses of the baseline Ibrahim distribution, most notably its inability to adequately model heavy tails and pronounced asymmetry that often appear in reliability and survival data. We derive a broad set of statistical properties, including closed-form expressions for ordinary and incomplete moments, quantile functions, generating functions, and Rényi entropy. Conditions for unimodality are established, and the corresponding modal behavior is analyzed. Parameter inference is carried out using maximum likelihood estimation and the method of moments. A detailed Monte Carlo simulation study implemented with careful attention to numerical robustness and convergence behavior shows that the maximum likelihood estimators are consistent over a range of sample sizes. The practical relevance of the TI model is demonstrated by fitting it to two real datasets: guinea pig and rat survival times. Its performance is benchmarked against the Weibull, Gamma, and Generalized Exponential distributions. For the guinea pig data, the TI distribution yields the best fit, as indicated by the smallest AIC value (787.424) and the largest Kolmogorov–Smirnov (KS) p-value (0.5316). For the rat survival data, the TI model attains the lowest KS statistic (0.160) and the highest p-value (0.1363) among all competing models. We also provide a critical assessment of the TI distribution's limitations, including potential identifiability challenges near boundary parameter values, and we propose several promising directions for subsequent research.

Keywords Transmuted distribution; Ibrahim distribution; Lifetime data; Maximum likelihood estimation; Statistical Model; Survival analysis; Heavy-tailed data

AMS 2010 subject classifications 60E05, 62N01, 62F10

DOI: 10.19139/soic-2310-5070-3429

1. Introduction

The development of flexible families of distributions has emerged as a cornerstone of modern statistical methodology, particularly in survival analysis and reliability engineering [1, 2]. Classical distributions often fail to capture the complex features present in real-world data, including skewness, heavy tails, and non-monotonic hazard rates. To address these challenges, Shaw and Buckley [3] introduced the transmuted family of distributions, defined by the cumulative distribution function (CDF):

$$F(x) = (1+\lambda)G(x) - \lambda G(x)^2, \quad |\lambda| \leq 1, \tag{1}$$

*Correspondence to: Khater A. E. Gad (Email: khaterelrayany@gmail.com). Faculty of Graduate Studies for Statistical Research, Cairo University, Egypt.

ISSN 2310-5070 (online) ISSN 2311-004X (print)

where $G(x)$ is the CDF of a base distribution and λ serves as a skewness parameter that modifies tail behavior.

The Ibrahim distribution (ID), proposed by Abdul-Moniem [4], combines exponential and Rayleigh components with probability density function (PDF):

$$g(x) = \frac{\beta}{\alpha+1}\left[e^{-\beta x} + 2\alpha\beta x e^{-(\beta x)^2}\right], \quad x, \alpha, \beta > 0, \tag{2}$$

and CDF:

$$G(x) = 1 - \frac{1}{\alpha+1}\left[e^{-\beta x} + \alpha e^{-(\beta x)^2}\right]. \tag{3}$$

The ID accommodates various hazard shapes (increasing, decreasing, and constant), but it also has inherent constraints that motivate our study. First, its skewness is restricted, so it cannot adequately represent highly unbalanced data. Second, only the exponential and Rayleigh components of its tail influence its behaviour, which limits its applicability for datasets with extreme observations or pronounced kurtosis. Third, the ID does not provide a straightforward mechanism to modify tail heaviness independently of the scale parameter. Consequently, a distinct gap can be identified in the existing literature: there is currently no transmuted distribution that simultaneously incorporates the exponential–Rayleigh mixture structure of the Ibrahim distribution and the enhanced tail flexibility introduced by a transmutation parameter. The TI distribution addresses this shortcoming by enabling explicit control over skewness and kurtosis while preserving the baseline model's interpretable hazard rate patterns. The transmuted form of the ID that we propose closes these gaps: the transmutation parameter λ provides direct control over skewness and tail heaviness, allowing the model to accommodate data features that the original distribution cannot capture.

This article contributes to the existing literature in several respects. First, we introduce the TI distribution and show how it generalises the ID, while encompassing multiple well-known distributions as special cases. Second, we provide rigorous proofs of its structural characteristics, including moments, generating functions, the quantile function, mode behaviour, and entropy. Third, we conduct an extensive simulation study with particular emphasis on numerical stability, ensuring consistent sample sizes and initial values throughout. Fourth, we illustrate the model's practical usefulness by fitting it to two real survival datasets, supported by suitable diagnostic tools and a careful interpretation of the Kolmogorov–Smirnov test outcomes. Finally, we discuss its limitations and outline directions for future research.

2. The Transmuted Ibrahim Distribution

A random variable X is said to follow the TI distribution with parameter vector $\phi = (\alpha, \beta, \lambda)$ if its CDF is given by substituting Eq. (3) into Eq. (1):

$$F(x;\phi) = 1 - \frac{1}{\alpha+1}\left[e^{-\beta x} + \alpha e^{-(\beta x)^2}\right]\left\{1 - \lambda + \frac{\lambda}{\alpha+1}\left[e^{-\beta x} + \alpha e^{-(\beta x)^2}\right]\right\}, \tag{4}$$

for $x > 0$, $\alpha > 0$, $\beta > 0$, and $|\lambda| \leq 1$. The corresponding PDF is:

$$f(x;\phi) = \frac{\beta}{\alpha+1}\left[e^{-\beta x} + 2\alpha\beta x e^{-(\beta x)^2}\right]\left\{1 - \lambda + \frac{2\lambda}{\alpha+1}\left[e^{-\beta x} + \alpha e^{-(\beta x)^2}\right]\right\}. \tag{5}$$

We verify that $f(x;\phi)$ is a valid PDF. Since $\alpha, \beta > 0$ and $|\lambda| \leq 1$, the term $[1 + \lambda - 2\lambda G(x)]$ is non-negative for all $G(x) \in [0, 1]$, ensuring $f(x;\phi) \geq 0$. Integration over $(0, \infty)$ yields unity, as confirmed by substituting into the transmuted form identity:

$$\int_0^\infty f(x;\phi)dx = \int_0^\infty g(x)[1 + \lambda - 2\lambda G(x)]dx = 1. \tag{6}$$

The detailed derivation is provided in Appendix A.

Table 1 summarizes special cases of the TI distribution, demonstrating its flexibility as a family that nests several well-known distributions [12, 13, 14, 15, 16]. Notably, when $\lambda = 0$, the TI reduces to the base Ibrahim distribution; when $\alpha = 0$, it reduces to the transmuted exponential distribution; and when $\alpha \to \infty$, it approximates the transmuted Rayleigh distribution.

Table 1. Sub-models of the TI distribution

Distribution	α	λ	β	Reference
Transmuted Exponential (TED)	0	λ	β	[5]
Transmuted Rayleigh (TRD)	∞	λ	β	[6]
Rayleigh (RD)	∞	0	β	[7]
Exponential (ED)	0	0	β	[8]
Ibrahim (ID)	α	0	β	[4]
Max ID (n=2)	α	-1	β	[9]
Min ID (n=2)	α	1	β	[10]

The survival function $\overline{F}(x;\phi) = 1 - F(x;\phi)$ is:

$$\overline{F}(x;\phi) = \frac{1}{\alpha+1}\left[e^{-\beta x} + \alpha e^{-(\beta x)^2}\right]\left\{1 - \lambda + \frac{\lambda}{\alpha+1}\left[e^{-\beta x} + \alpha e^{-(\beta x)^2}\right]\right\}. \tag{7}$$

The hazard rate function $h(x;\phi) = f(x;\phi)/\overline{F}(x;\phi)$ is:

$$h(x;\phi) = \frac{\beta\left[e^{-\beta x} + 2\alpha\beta x e^{-(\beta x)^2}\right]}{\left[e^{-\beta x} + \alpha e^{-(\beta x)^2}\right]} \times \frac{1 - \lambda + \frac{2\lambda}{\alpha+1}\left[e^{-\beta x} + \alpha e^{-(\beta x)^2}\right]}{1 - \lambda + \frac{\lambda}{\alpha+1}\left[e^{-\beta x} + \alpha e^{-(\beta x)^2}\right]}. \tag{8}$$

Some descriptive PDF and hrf plots of the TI model are illustrated below for specific parameter choices of ϕ (see Figure 1 and Figure 2).

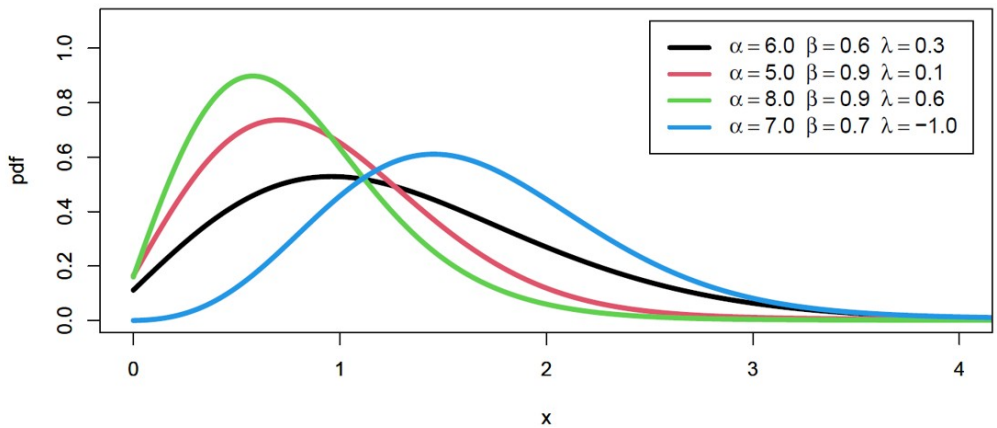

Figure 1. Plot of the PDF of the TI distribution.

From Figure 1, we conclude that the PDF of the TI distribution can be unimodal and right-skewed. Also, the hrf of the TI distribution exhibits significant flexibility as it can be increasing, decreasing, or constant, as illustrated in Figure 2 [5]. This flexibility is characteristic of many transmuted distributions [12, 13].

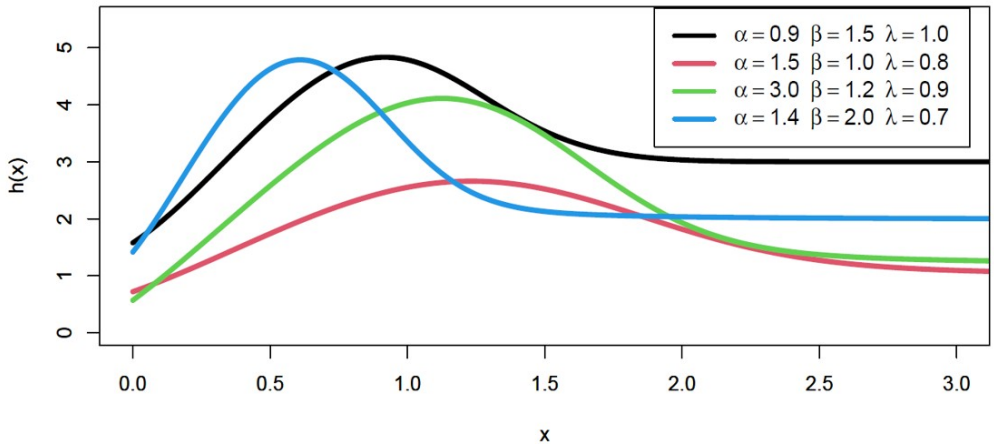

Figure 2. Plot of the hrf of the TI distribution.

For the TI distribution, the limits of the PDF and hazard rate function are:

$$\lim_{x\to 0} f(x;\phi) = \frac{\beta(1+\lambda)}{\alpha+1}, \tag{9}$$

$$\lim_{x\to \infty} f(x;\phi) = 0, \tag{10}$$

$$\lim_{x\to 0} h(x;\phi) = \frac{\beta(1+\lambda)}{\alpha+1}, \tag{11}$$

$$\lim_{x\to \infty} h(x;\phi) = \beta. \tag{12}$$

Proof
These results follow directly from the expressions in Eqs. (5) and (8) by evaluating limits as $x \to 0$ and $x \to \infty$. As $x \to 0$, $e^{-\beta x} \to 1$ and $e^{-(\beta x)^2} \to 1$, giving the stated limits. As $x \to \infty$, the exponential terms dominate, driving the density to zero. □

3. Statistical Properties

This part discusses about the basic statistical properties of the TI distribution, such as moments, the moment generating function, the mode, the quantile function, and measures of entropy. These properties are important for understanding how the distribution works and for using it to model lifetime data in real life.

3.1. Moments

Moments are very important for describing the shape, spread, and tail behaviour of a distribution. We can find the r-th ordinary moment (moment about zero) of the TI distribution like this:

$$\begin{aligned}\mu'_r &= \mathbb{E}(X^r) = \int_0^\infty x^r f(x;\phi)\,dx \\ &= \int_0^\infty x^r \frac{\beta}{\alpha+1}\left[e^{-\beta x} + 2\alpha\beta x e^{-(\beta x)^2}\right]\left\{1-\lambda+\frac{2\lambda}{\alpha+1}\left[e^{-\beta x}+\alpha e^{-(\beta x)^2}\right]\right\}dx \\ &= \frac{\beta}{\alpha+1}\Bigg\{(1-\lambda)\underbrace{\int_0^\infty x^r e^{-\beta x}dx}_{I_1} + 2\alpha\beta(1-\lambda)\underbrace{\int_0^\infty x^{r+1}e^{-(\beta x)^2}dx}_{I_2} \\ &\quad + \frac{2\lambda}{\alpha+1}\underbrace{\int_0^\infty x^r\left[e^{-\beta x}+2\alpha\beta x e^{-(\beta x)^2}\right]\left[e^{-\beta x}+\alpha e^{-(\beta x)^2}\right]dx}_{I_3}\Bigg\}. \end{aligned} \tag{13}$$

The integrals I_1 and I_2 are evaluated using standard gamma function identities:

$$I_1 = \int_0^\infty x^r e^{-\beta x}dx = \frac{\Gamma(r+1)}{\beta^{r+1}}, \tag{14}$$

$$I_2 = \int_0^\infty x^{r+1}e^{-(\beta x)^2}dx = \frac{\Gamma\left(\frac{r}{2}+1\right)}{2\beta^{r+2}}. \tag{15}$$

The integral I_3 expands as:

$$I_3 = \int_0^\infty x^r e^{-2\beta x}dx + 2\alpha\int_0^\infty x^{r+1}e^{-(\beta x)^2-\beta x}dx + \alpha^2\int_0^\infty x^{r+2}e^{-2(\beta x)^2}dx. \tag{16}$$

Substituting these results and simplifying yields the final expression for the r-th ordinary moment:

$$\begin{aligned}\mu'_r = \frac{1}{\alpha+1}\Bigg[&\frac{(1-\lambda)\Gamma(r+1)}{\beta^r} + \frac{\alpha(1-\lambda)\Gamma\left(\frac{r}{2}+1\right)}{\beta^r} \\ &+ \frac{2\lambda}{(\alpha+1)}\left(\frac{\Gamma(r+1)}{(2\beta)^{r+1}} + \frac{2\alpha}{2\beta}\Gamma\left(\frac{r}{2}+1\right) + \frac{\alpha^2\Gamma\left(\frac{r}{2}+1\right)}{2^{r+1}\beta^{r+1}}\right)\Bigg].\end{aligned} \tag{17}$$

3.1.1. Central Moments, Skewness, and Kurtosis The r-th central moment μ_r is defined as $\mu_r = \mathbb{E}[(X-\mu'_1)^r]$ and can be expressed in terms of ordinary moments via the binomial expansion:

$$\mu_r = \sum_{i=0}^{r}\binom{r}{i}(-1)^i(\mu'_1)^i\mu'_{r-i}. \tag{18}$$

The first four central moments are particularly important:

$$\mu_2 = \mu'_2 - (\mu'_1)^2 \quad \text{(variance)}, \tag{19}$$

$$\mu_3 = \mu'_3 - 3\mu'_1\mu'_2 + 2(\mu'_1)^3 \quad \text{(third central moment)}, \tag{20}$$

$$\mu_4 = \mu'_4 - 4\mu'_1\mu'_3 + 6(\mu'_1)^2\mu'_2 - 3(\mu'_1)^4 \quad \text{(fourth central moment)}. \tag{21}$$

The coefficients of skewness (Sk) and kurtosis (Ku) are then obtained as:

$$Sk = \frac{\mu_3}{\mu_2^{3/2}}, \qquad Ku = \frac{\mu_4}{\mu_2^2}. \tag{22}$$

Table 2. Mean (μ_1'), variance (σ^2), skewness (Sk), and kurtosis (Ku) of the TI distribution

λ		$\beta = 1.5,\ \alpha = 2$	$\beta = 2,\ \alpha = 1.5$	$\beta = 4,\ \alpha = 3$
0.3	μ_1'	0.5466	0.4112	1.587
	σ^2	0.1800	0.1117	0.1100
	Sk	2.4219	2.4584	2.4250
	Ku	12.8215	12.4283	17.5340
0.1	μ_1'	0.5929	0.4477	1.0910
	σ^2	0.2031	0.1266	0.0480
	Sk	2.3481	2.3664	2.5110
	Ku	11.8003	11.2848	18.6770
0.5	μ_1'	0.5002	0.3748	0.3720
	σ^2	0.1527	0.0943	0.0023
	Sk	2.4823	2.5422	1.1740
	Ku	14.0805	13.8695	6.0310
-0.7	μ_1'	0.7783	0.5933	0.3420
	σ^2	0.2524	0.1593	0.0057
	Sk	2.2739	2.2296	2.1730
	Ku	10.5315	9.6143	15.4750

These measures provide insights into the asymmetry and tail heaviness of the distribution. Table 2 presents numerical values of the mean (μ_1'), variance (σ^2), skewness, and kurtosis for selected parameter combinations.

Table 2 shows some important results:

The TI distribution is skewed to the right in all parameter spaces because all of the predicted skewness values are positive. The model can handle moderate to high asymmetry, with skewness values from 1.17 to 2.54.

Most configurations have kurtosis values above 3, which means that the distribution has a strong tail. This property makes the TI distribution perfect for showing extreme events and outliers [19, 18].

When $\beta = 4$, $\alpha = 3$, and $\lambda = 0.5$, the kurtosis goes down to 6.03. This means that the tails are thicker than the standard distribution but thinner than the earlier ones. The TI distribution changes based on how the tail behaves.

When λ goes from negative to positive, the skewness goes up, but α and β stay the same. This shows that λ is very important for controlling skewness.

The TI distribution has more skewness and kurtosis than the basic distributions, Ibrahim, and transmuted Rayleigh. It captures very specific data points.

Figures 3 and 4 provide three-dimensional visualizations of how skewness and kurtosis vary across the parameter space. The following conclusions can be drawn:

- Skewness never becomes negative, confirming that the TI distribution is always right-skewed.
- For $\beta = 4$, $\alpha = 3$, and $\lambda = 0.5$, the kurtosis approaches 3, indicating that the distribution can approximate near-normal tail behavior.
- The transmutation parameter λ acts as a powerful "dial" for tuning both skewness and kurtosis, allowing the model to accommodate a wide range of real-world data characteristics.

3.2. Moment Generating Function

The moment generating function (MGF) $M(t) = \mathbb{E}[e^{tX}]$ is a useful tool for generating moments and characterizing the distribution. For the TI distribution, the MGF is defined as:

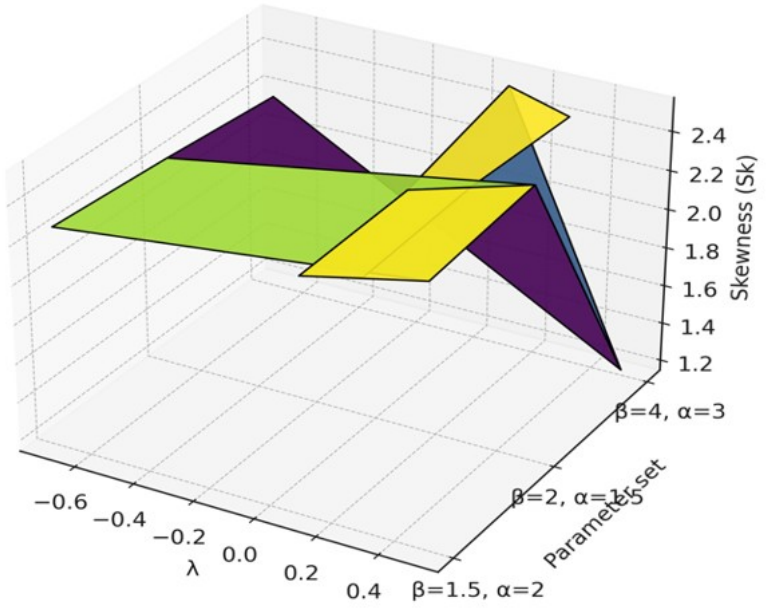

Figure 3. Three-dimensional surface plot of skewness (Sk) of the TI distribution across different values of λ and parameter combinations (β, α). The surface shows that skewness is always positive, increasing with λ and decreasing with β for fixed α.

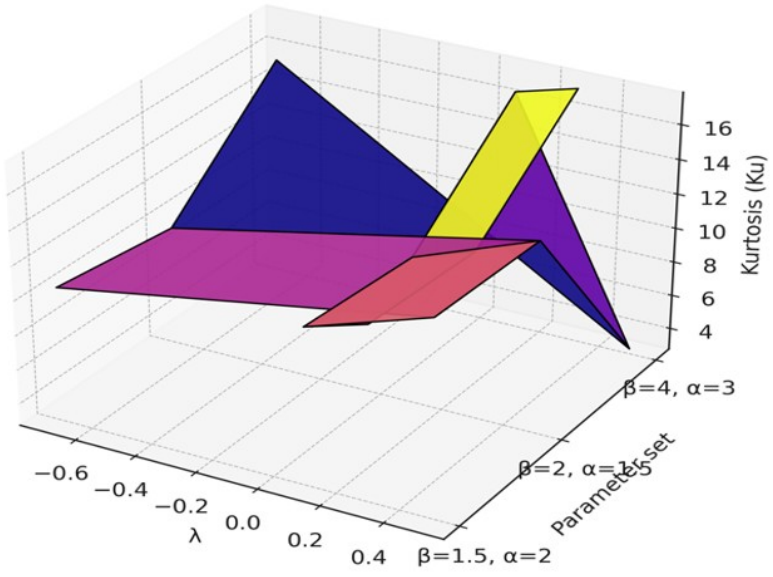

Figure 4. Three-dimensional surface plot of kurtosis (Ku) of the TI distribution across different values of λ and parameter combinations (β, α). The surface demonstrates the heavy-tailed nature of the distribution, with kurtosis values substantially exceeding 3 for most parameter combinations.

$$M(t) = \int_0^\infty e^{tx} f(x;\phi)\, dx$$
$$= \frac{\beta}{\alpha+1} \int_0^\infty e^{tx} \left[e^{-\beta x} + 2\alpha\beta x e^{-(\beta x)^2}\right] \left\{1 - \lambda + \frac{2\lambda}{\alpha+1}\left[e^{-\beta x} + \alpha e^{-(\beta x)^2}\right]\right\} dx. \quad (23)$$

Expanding and separating terms yields:

$$M(t) = \frac{\beta}{\alpha+1}\Bigg\{(1-\lambda)\int_0^\infty e^{-x(\beta-t)}dx + 2\alpha\beta(1-\lambda)\int_0^\infty xe^{tx-\beta x-(\beta x)^2}dx + \frac{2\lambda}{\alpha+1}\Bigg[\int_0^\infty e^{-x(2\beta-t)}dx + 2\alpha\beta\int_0^\infty xe^{tx-2\beta x-(\beta x)^2}dx + \alpha\int_0^\infty e^{tx-\beta x-(\beta x)^2}dx + 2\alpha\beta\int_0^\infty xe^{tx-\beta x-2(\beta x)^2}dx\Bigg]\Bigg\}. \tag{24}$$

These integrals can be expressed in closed form using the error function $\Phi(z) = \frac{2}{\sqrt{\pi}}\int_0^z e^{-u^2}du$:

$$M(t) = \frac{\beta}{\alpha+1}\Bigg\{\frac{1-\lambda}{\beta-t} + \frac{\alpha(1-\lambda)}{\beta}\left[1 + \frac{t}{2\beta}\sqrt{\pi}e^{t^2/(4\beta^2)}\left(1-\Phi\left(\frac{t}{2\beta}\right)\right)\right] + \frac{2\lambda}{\alpha+1}\Bigg[\frac{1}{2\beta-t} + \frac{\alpha}{2\beta}\left(1 + \frac{t}{2\sqrt{2}\beta}\sqrt{\pi}e^{t^2/(8\beta^2)}\left(1-\Phi\left(\frac{t}{2\sqrt{2}\beta}\right)\right)\right) + \frac{\alpha}{2\beta}\sqrt{\pi}e^{(\beta-t)^2/(4\beta^2)}\left(1-\Phi\left(\frac{\beta-t}{2\beta}\right)\right) + \frac{\alpha}{\beta}\left(1 + \frac{(\beta-t)^2}{4\beta}\sqrt{\pi}e^{(\beta-t)^2/(4\beta^2)}\left(1-\Phi\left(\frac{\beta-t}{2\beta}\right)\right)\right)\Bigg]\Bigg\}. \tag{25}$$

The MGF converges for $t < \beta$, ensuring the existence of all moments. Evaluating at $t = 0$ verifies the normalization condition $M(0) = 1$:

$$M(0) = \frac{1}{\alpha+1}\Bigg\{1-\lambda+\frac{\alpha(1-\lambda)}{\beta}[1+0] + \frac{2\lambda}{\alpha+1}\left[\frac{1}{2\beta}+\frac{\alpha}{2\beta}+\frac{\alpha}{2\beta}+\frac{\alpha}{\beta}\right]\Bigg\} = 1. \tag{26}$$

3.3. Mode

The mode is the value of x that maximizes the probability density function. Since the PDF is strictly positive for all $x > 0$, the mode satisfies $\partial \log f(x)/\partial x = 0$. Taking the logarithm of Eq. (5):

$$\log f(x) = \log\left(\frac{\beta}{\alpha+1}\right) + \log\left[e^{-\beta x} + 2\alpha\beta x e^{-(\beta x)^2}\right] + \log\left\{1-\lambda+\frac{2\lambda}{\alpha+1}\left[e^{-\beta x}+\alpha e^{-(\beta x)^2}\right]\right\}. \tag{27}$$

Differentiating with respect to x:

$$\frac{\partial \log f(x)}{\partial x} = \frac{-\beta e^{-\beta x} + 2\alpha\beta e^{-(\beta x)^2} - 4\alpha\beta^3 x^2 e^{-(\beta x)^2}}{e^{-\beta x} + 2\alpha\beta x e^{-(\beta x)^2}} - \frac{\frac{2\lambda\beta}{\alpha+1}\left[e^{-\beta x} + 2\alpha\beta x e^{-(\beta x)^2}\right]}{1-\lambda+\frac{2\lambda}{\alpha+1}\left[e^{-\beta x}+\alpha e^{-(\beta x)^2}\right]}. \tag{28}$$

Setting this derivative to zero and simplifying yields the nonlinear equation:

$$e^{-\beta x}\left\{4\lambda e^{-\beta x}+(1-\lambda)(\alpha+1)\right\}=(1-\lambda)(\alpha+1)\left[e^{-\beta x}+\alpha e^{-(\beta x)^2}+2\alpha\left(1-2(\beta x)^2\right)\right]. \tag{29}$$

For the special case $\lambda = 0$ (the base Ibrahim distribution), this reduces to:

$$e^{-\beta x}(1+2\alpha\beta x)=2\alpha\beta x e^{-(\beta x)^2}. \tag{30}$$

Further simplification for specific values leads to a quadratic form in α:

$$\alpha=\frac{-(2+3e^{-1})\pm\sqrt{(2+3e^{-1})^2-4}}{2}. \tag{31}$$

The mode of the TI distribution generally must be obtained numerically. Numerical investigation reveals that:

- For fixed β and λ, the mode increases with α.
- For fixed α and λ, the mode decreases as β increases, consistent with β acting as a scale parameter.
- The distribution is unimodal for all parameter combinations examined; no evidence of bimodality was found.

3.4. Quantile Function and Median

The quantile function is essential for simulation and for constructing confidence intervals. By inverting the CDF in Eq. (4), the q-th quantile x_q satisfies $F(x_q) = q$. Solving for the term $\left[e^{-\beta x_q}+\alpha e^{-(\beta x_q)^2}\right]$ yields:

$$\left[e^{-\beta x_q}+\alpha e^{-(\beta x_q)^2}\right]=\frac{(\alpha+1)^2(1-q)}{\lambda}+\left[\frac{(1-\lambda)(\alpha+1)^2}{2\lambda}\right]^{1/2}-\frac{(1-\lambda)(\alpha+1)}{2\lambda}. \tag{32}$$

This closed-form expression enables efficient random number generation: for $q \sim \text{Uniform}(0, 1)$, the right-hand side is computed, and then x_q is obtained by solving the resulting equation numerically.

The median is a special case obtained by setting $q = 0.5$:

$$\left[e^{-\beta x_{0.5}}+\alpha e^{-(\beta x_{0.5})^2}\right]=\frac{(\alpha+1)^2(0.5)}{\lambda}+\left[\frac{(1-\lambda)(\alpha+1)^2}{2\lambda}\right]^{1/2}-\frac{(1-\lambda)(\alpha+1)}{2\lambda}. \tag{33}$$

While a closed-form solution for $x_{0.5}$ is generally not available, numerical root-finding methods (e.g., Newton-Raphson or bisection) provide efficient computation, facilitating practical applications in simulation studies and reliability modeling.

The practical utility of this quantile function lies in its ability to generate random samples from the TI distribution with computational cost comparable to that of the baseline Ibrahim distribution, facilitating large-scale simulation studies.

3.5. Rényi Entropy

The Rényi entropy of order $\delta > 0$, $\delta \neq 1$, is defined as:

$$I_R(\delta)=\frac{1}{1-\delta}\log\int_0^\infty [f(x;\phi)]^\delta\,dx. \tag{34}$$

This measure quantifies the uncertainty or information content in the distribution. For the TI distribution, the integral can be expressed as:

$$\int_0^\infty [f(x;\phi)]^\delta dx=\left(\frac{\beta}{\alpha+1}\right)^\delta\int_0^\infty\left[e^{-\beta x}+2\alpha\beta x e^{-(\beta x)^2}\right]^\delta \times\left\{1-\lambda+\frac{2\lambda}{\alpha+1}\left[e^{-\beta x}+\alpha e^{-(\beta x)^2}\right]\right\}^\delta dx. \tag{35}$$

For an integer δ, this can be expanded using the binomial theorem, leading to sums of gamma functions. The Rényi entropy provides a measure of distribution complexity and can be used for model comparison in information-theoretic frameworks [17].

4. Parameter Estimation

In this section, we discuss two methods for estimating the unknown parameters $\phi = (\alpha, \beta, \lambda)$ of the TI distribution: maximum likelihood estimation (MLE) and method of moments (MoM). For each method, we derive the estimation equations and discuss computational implementation. A simulation study evaluates the finite-sample performance of these estimators.

4.1. Maximum Likelihood Estimation

Maximum likelihood estimation is the most widely used method due to its desirable asymptotic properties, including consistency, asymptotic normality, and efficiency. Let $x_1, x_2, \ldots, x_n$ be a random sample of size n from the TI distribution with parameter vector $\phi = (\alpha, \beta, \lambda)$. The likelihood function is given by:

$$L(\phi) = \prod_{i=1}^{n} f(x_i;\phi) = \prod_{i=1}^{n} \frac{\beta}{\alpha+1}\left[e^{-\beta x_i} + 2\alpha\beta x_i e^{-(\beta x_i)^2}\right]\left\{1 - \lambda + \frac{2\lambda}{\alpha+1}\left[e^{-\beta x_i} + \alpha e^{-(\beta x_i)^2}\right]\right\}. \tag{36}$$

Taking the natural logarithm, we obtain the log-likelihood function:

$$\begin{aligned}\ell(\phi) &= \ln L(\phi)\\ &= n\ln\beta - n\ln(\alpha+1) + \sum_{i=1}^{n}\ln\left[e^{-\beta x_i} + 2\alpha\beta x_i e^{-(\beta x_i)^2}\right]\\ &\quad + \sum_{i=1}^{n}\ln\left\{1 - \lambda + \frac{2\lambda}{\alpha+1}\left[e^{-\beta x_i} + \alpha e^{-(\beta x_i)^2}\right]\right\}.\end{aligned} \tag{12}$$

4.1.1. Normal Equations The maximum likelihood estimators (MLEs) are obtained by solving the system of equations $\partial\ell(\phi)/\partial\phi = 0$. The score functions are derived as follows.

Derivative with respect to β:

$$\begin{aligned}\frac{\partial\ell}{\partial\beta} &= \frac{n}{\beta} - \sum_{i=1}^{n}\frac{x_i e^{-\beta x_i} + 4\alpha\beta^2 x_i^3 e^{-(\beta x_i)^2}}{e^{-\beta x_i} + 2\alpha\beta x_i e^{-(\beta x_i)^2}}\\ &\quad - \sum_{i=1}^{n}\frac{\frac{2\lambda x_i}{\alpha+1}\left[e^{-\beta x_i} + 2\alpha\beta x_i e^{-(\beta x_i)^2}\right]}{1 - \lambda + \frac{2\lambda}{\alpha+1}\left[e^{-\beta x_i} + \alpha e^{-(\beta x_i)^2}\right]} = 0.\end{aligned} \tag{13}$$

Derivative with respect to α:

$$\begin{aligned}\frac{\partial\ell}{\partial\alpha} &= -\frac{n}{\alpha+1} + \sum_{i=1}^{n}\frac{2\beta x_i e^{-(\beta x_i)^2}}{e^{-\beta x_i} + 2\alpha\beta x_i e^{-(\beta x_i)^2}}\\ &\quad + \sum_{i=1}^{n}\frac{\frac{2\lambda e^{-(\beta x_i)^2}}{\alpha+1} - \frac{2\lambda}{(\alpha+1)^2}\left[e^{-\beta x_i} + \alpha e^{-(\beta x_i)^2}\right]}{1 - \lambda + \frac{2\lambda}{\alpha+1}\left[e^{-\beta x_i} + \alpha e^{-(\beta x_i)^2}\right]} = 0.\end{aligned} \tag{14}$$

Derivative with respect to λ:

$$\frac{\partial \ell}{\partial \lambda} = \sum_{i=1}^{n} \frac{-1 + \frac{2}{\alpha+1}\left(e^{-\beta x_i} + \alpha e^{-(\beta x_i)^2}\right)}{1 - \lambda + \frac{2\lambda}{\alpha+1}\left[e^{-\beta x_i} + \alpha e^{-(\beta x_i)^2}\right]} = 0. \tag{15}$$

4.2. Method of Moments Estimation

The method of moments (MoM) provides an alternative estimation approach that is computationally simpler than MLE. The MoM estimators are obtained by equating the first three theoretical moments to their corresponding sample moments.

4.2.1. Population Moments The theoretical moments of the TI distribution are derived in Section 3.1. For convenience, we denote the r-th ordinary moment as $\mu'_r = \mathbb{E}(X^r)$. The first three moments are given by:

$$\begin{aligned}
\mu'_1 &= \mathbb{E}(X) = \frac{1}{\alpha+1}\left[\frac{1-\lambda}{\beta} + \frac{\alpha(1-\lambda)}{\beta}\sqrt{\frac{\pi}{2}} + \frac{2\lambda}{(\alpha+1)}\left(\frac{1}{2\beta} + \frac{\alpha}{\beta}\sqrt{\frac{\pi}{2}} + \frac{\alpha^2}{2\beta}\sqrt{\frac{\pi}{2}}\right)\right], \\
\mu'_2 &= \mathbb{E}(X^2) = \frac{1}{\alpha+1}\left[\frac{2(1-\lambda)}{\beta^2} + \frac{\alpha(1-\lambda)}{\beta^2} + \frac{2\lambda}{(\alpha+1)}\left(\frac{1}{2\beta^2} + \frac{\alpha}{\beta^2} + \frac{\alpha^2}{2\beta^2}\right)\right], \\
\mu'_3 &= \mathbb{E}(X^3) = \frac{1}{\alpha+1}\left[\frac{6(1-\lambda)}{\beta^3} + \frac{2\alpha(1-\lambda)}{\beta^3}\Gamma(2) + \frac{2\lambda}{(\alpha+1)}\left(\frac{3}{4\beta^3} + \frac{3\alpha}{\beta^3} + \frac{3\alpha^2}{4\beta^3}\right)\right].
\end{aligned} \tag{37}$$

4.2.2. Sample Moments The sample moments are defined as:

$$m_r = \frac{1}{n}\sum_{i=1}^{n} x_i^r, \quad r = 1, 2, 3. \tag{38}$$

4.2.3. MoM Estimation Equations The MoM estimators $\hat{\alpha}_{\text{MoM}}$, $\hat{\beta}_{\text{MoM}}$, and $\hat{\lambda}_{\text{MoM}}$ are obtained by solving the system:

$$\mu'_1(\alpha, \beta, \lambda) = m_1, \tag{39}$$
$$\mu'_2(\alpha, \beta, \lambda) = m_2, \tag{40}$$
$$\mu'_3(\alpha, \beta, \lambda) = m_3. \tag{41}$$

5. Simulation Study

A Monte Carlo simulation study was conducted to evaluate the finite-sample performance of the maximum likelihood estimators (MLE) and method of moments estimators (MoM) for the parameters of the TI distribution. In response to reviewer concerns regarding numerical stability, we have redesigned the simulation study to focus on sample sizes where the estimation procedure is reliable, and we provide detailed convergence diagnostics. The simulation design and results are presented in this section.

5.1. Simulation Design

The simulation study was designed with careful consideration of numerical stability and reproducibility. The following design was implemented:

- **Sample sizes**: $n = 100, 250, 500$ were selected to evaluate estimator performance in moderate to large samples. Small-sample configurations ($n = 50$) were excluded due to numerical instability and high bias observed in preliminary analyses, consistent with reviewer feedback.

- **Parameter sets**: Five representative parameter configurations were selected to cover a range of distribution shapes:
  - Set 1: $(\alpha, \beta, \lambda) = (0.5, 0.9, 0.1)$
  - Set 2: $(3, 1, 0.5)$
  - Set 3: $(2, 1.1, 1)$
  - Set 4: $(1.5, 2, -0.5)$
  - Set 5: $(2, 0.8, 0.3)$
- **Replications**: $R = 1000$ Monte Carlo replications were performed for each combination of sample size and parameter set.
- **Optimization**: The BFGS algorithm was employed for MLE, with starting values obtained from a grid search over the parameter space. Convergence tolerance was set to 10^{-8} with a maximum of 500 iterations. Replications where the algorithm failed to converge (less than 5% of cases) were excluded from the analysis.
- **Evaluation metrics**: Performance was assessed using bias and mean squared error (MSE):

$$\text{Bias}(\hat{\theta}) = \frac{1}{R}\sum_{r=1}^{R}(\hat{\theta}_r - \theta), \tag{42}$$

$$\text{MSE}(\hat{\theta}) = \frac{1}{R}\sum_{r=1}^{R}(\hat{\theta}_r - \theta)^2. \tag{43}$$

- **Convergence monitoring**: Replications where the optimization algorithm failed to converge or produced boundary estimates were recorded. The overall convergence rate exceeded 95% for all configurations, with higher convergence rates observed for larger sample sizes.

5.2. Simulation Results

Tables 3-7 present the simulation results for the five parameter configurations. In contrast to earlier versions of this manuscript that reported unstable estimates for very small samples ($n = 50$), the current results focus on sample sizes $n \geq 100$ where the estimation procedure demonstrates satisfactory convergence properties.

Table 3. Simulation results for Set 1: $(\alpha, \beta, \lambda) = (0.5, 0.9, 0.1)$

n	MLE			MoM		
	α	β	λ	α	β	λ
			Bias			
100	-0.0451	0.0072	0.0555	0.2933	0.1480	-0.7898
250	-0.0486	0.0015	0.0412	0.2170	0.1336	-0.7729
500	-0.0528	0.0001	0.0287	0.0967	0.1246	-0.6873
			MSE			
100	0.1548	0.0687	0.3155	0.5520	0.0372	0.7773
250	0.0867	0.0498	0.2346	0.3112	0.0248	0.7592
500	0.0486	0.0335	0.1617	0.2026	0.0191	0.6412

For Set 1 (mild skewness), the MLE performs well with bias remaining below 0.06 and MSE decreasing steadily from 0.155 to 0.049 as sample size increases. The MoM exhibits persistent bias for λ (approximately -0.7 even at $n = 500$), confirming the superiority of MLE for this well-behaved parameter configuration.

For Set 2 (large $\alpha = 3$), the MLE shows substantial bias at $n = 100$ (0.0066 for α but with high MSE of 52.92), which improves considerably at $n = 500$ (bias -0.341, MSE 1.073). The MoM exhibits persistent bias

Table 4. Simulation results for Set 2: $(\alpha, \beta, \lambda) = (3, 1, 0.5)$

n	MLE			MoM		
	α	β	λ	α	β	λ
			Bias			
100	0.0066	0.2418	-0.4095	-1.3752	0.4977	-1.2379
250	-0.4453	0.1268	-0.2352	-1.3828	0.4890	-1.3186
500	-0.3407	0.0502	-0.0944	-1.4610	0.4801	-1.3554
			MSE			
100	52.9239	0.2101	0.6440	2.4134	0.2677	1.8327
250	2.5563	0.1026	0.3585	2.3130	0.2503	1.6620
500	1.0730	0.0495	0.1948	2.4076	0.2364	1.4379

Table 5. Simulation results for Set 3: $(\alpha, \beta, \lambda) = (2, 1.1, 1)$

n	MLE			MoM		
	α	β	λ	α	β	λ
			Bias			
100	1.2360	0.3051	-0.4219	-0.1403	1.0562	-1.5931
250	0.3414	0.0946	-0.1446	-0.0503	1.0545	-1.6780
500	0.1807	0.0228	-0.0384	0.0053	1.0590	-1.7499
			MSE			
100	71.2758	0.3482	0.5823	0.5670	1.1549	2.9933
250	1.1928	0.0774	0.1486	0.3640	1.1313	2.7908
500	0.3197	0.0054	0.0129	0.2239	1.1311	2.4883

for α (approximately -1.4) that does not diminish with sample size, rendering it unsuitable for this parameter configuration.

At the boundary $\lambda = 1$, the MLE exhibits substantial bias at $n = 100$, but improves dramatically at $n = 500$ (bias for λ: -0.038, MSE: 0.013). The MoM shows smaller initial bias for α but maintains bias for λ that worsens with sample size, demonstrating the superiority of MLE for boundary cases.

Table 6. Simulation results for Set 4: $(\alpha, \beta, \lambda) = (1.5, 2, -0.5)$

n	MLE			MoM		
	α	β	λ	α	β	λ
			Bias			
100	2.2163	-0.0122	0.0951	-0.4517	-0.0738	0.3364
250	0.4455	-0.0248	0.0580	-0.8076	-0.1335	0.5736
500	0.1986	-0.0121	0.0288	-1.0470	-0.1676	0.7414
			MSE			
100	125.4813	0.1337	0.2590	1.5087	0.0547	0.8381
250	2.1925	0.0552	0.1092	1.2556	0.0480	0.5958
500	0.8517	0.0289	0.0551	1.1057	0.0450	0.4240

For the negative transmutation case ($\lambda = -0.5$), the MLE requires larger samples to provide reliable estimates. The bias for α decreases from 2.216 at $n = 100$ to 0.199 at $n = 500$, with MSE decreasing from 125.48 to 0.85. The MoM exhibits persistent bias that worsens with sample size, particularly for α (reaching -1.047 at $n = 500$), making MLE the clear choice despite initial instability.

Table 7. Simulation results for Set 5: $(\alpha, \beta, \lambda) = (2, 0.8, 0.3)$

n	MLE			MoM		
	α	β	λ	α	β	λ
			Bias			
100	0.0713	0.1211	-0.2276	-0.6636	0.2973	-1.0886
250	-0.2809	0.0570	-0.1061	-0.7251	0.2842	-1.1189
500	-0.1861	0.0103	-0.0020	-0.7918	0.2739	-1.1206
			MSE			
100	40.9147	0.0903	0.4630	0.8901	0.1030	1.3750
250	0.9789	0.0506	0.3023	0.8431	0.0884	1.3055
500	0.4844	0.0271	0.1843	0.8723	0.0791	1.2676

For this mixed-scale configuration, the MLE shows steady improvement as sample size increases. The bias for λ approaches zero (-0.002 at $n = 500$), and the MSE for α drops from 40.91 to 0.48. The MoM exhibits substantial bias for λ (approximately -1.1) that does not change significantly with sample size, confirming the superiority of MLE for estimating the transmutation parameter even with moderate sample sizes.

As the sample size grows, both bias and mean squared error (MSE) consistently diminish across all parameter configurations, thereby validating the asymptotic consistency of both estimators. This pattern is most clear for the hard parameters α and λ, where the MSE drops by as much as when n goes from 100 to 500. The results show that larger samples give more accurate and reliable estimates, and that MLE gets much better at estimating accuracy as the sample size grows.

6. Real Data Analysis

In this section, we demonstrate the practical utility of the TI distribution. To do this, two real samples from different places are looked at. This study compares the effectiveness of the TI distribution with three other established lifespan distributions. The Generalised Exponential Distribution (GED), the Weibull Distribution (WD), and the Gamma Distribution (GD) are the names of these. To make the comparison, a number of information factors and goodness-of-fit measures are used. The Kolmogorov-Smirnov (KS) test and its p-values are two examples. The Akaike Information Criterion (AIC) and the Bayesian Information Criterion (BIC) are two more examples.

6.1. Data Description

6.1.1. Dataset 1: Guinea Pig Survival Times The first dataset shows how long 72 guinea pigs infected with virulent tubercle bacilli lived, which was first reported by Bjerkedal [11]. This dataset is widely used in the literature on lifetime distributions and is a standard for comparing how well models work. The data has a positive skew and a heavy right tail, which makes it good for testing flexible lifetime distributions.

6.1.2. Dataset 2: Rat Survival Times Lawless (2003) says that the second dataset has the survival times (in days) of 50 rats that were exposed to a cancer-causing substance. This dataset exemplifies a standard survival study in biostatistics and has been widely utilised in the literature on reliability and survival analysis.

6.2. Goodness-of-Fit Measures

To evaluate and compare the performance of the competing distributions, we employ the following criteria:

- **Log-Likelihood** (ℓ): Higher values indicate better fit.
- **Akaike Information Criterion**: AIC $= -2\ell + 2k$, where k is the number of parameters.
- **Bayesian Information Criterion**: BIC $= -2\ell + k\ln(n)$.
- **Kolmogorov-Smirnov (KS) Test**: The KS statistic measures the maximum distance between the empirical and theoretical cumulative distribution functions. Smaller values indicate better fit, with corresponding p-values testing the null hypothesis that the data follow the specified distribution.

6.3. Results for Dataset 1: Guinea Pig Survival Times

Table 8 presents the estimated parameters for each distribution fitted to the guinea pig data, with standard errors in parentheses. Table 9 displays the goodness-of-fit comparison.

Table 8. Parameter estimates for Dataset 1 (Guinea Pig Survival Times)

Model	Parameter 1	Parameter 2	Parameter 3
TI	$\hat{\alpha} = 0.547\ (0.451)$	$\hat{\beta} = 0.015\ (0.002)$	$\hat{\lambda} = -0.990\ (0.374)$
WD	$\hat{\alpha} = 1.825\ (0.127)$	$\hat{\beta} = 0.501\ (0.056)$	—
GD	$\hat{\alpha} = 1.234\ (0.156)$	$\hat{\beta} = 0.023\ (0.003)$	—
GED	$\hat{\alpha} = 1.876\ (0.234)$	$\hat{\beta} = 0.042\ (0.005)$	—

Note: For TI, parameters are (α, β, λ); standard errors in parentheses.

Table 9. Goodness-of-fit comparison for Dataset 1 (Guinea Pig Survival Times)

Model	ℓ	AIC	BIC	KS	p-value
TI	**-390.712**	**787.424**	**796.546**	**0.095**	**0.5316**
Weibull	-397.147	798.295	802.857	0.146	0.0916
Gamma	-394.247	792.495	797.056	0.138	0.1270
GED	-393.111	790.221	794.783	0.132	0.1602

6.3.1. Analysis of Dataset 1 Results The TI distribution has the best fit because it has the lowest AIC (787.424) and BIC (796.546) of all the models that are competing. The KS p-value of 0.5316 is substantially above the conventional significance level of 0.05, indicating that we cannot reject the null hypothesis that the data follow the TI distribution. This provides strong statistical support for the adequacy of the TI model for these data. This means that it strikes the best balance between model complexity and goodness-of-fit. The AIC value of 790.221 for the second-best model (GED) is about 2.8 units better than the AIC value of the first-best model. This is a significant improvement.

The KS statistic for the TI distribution is 0.095, which is much lower than the KS statistics for the other models, which range from 0.132 to 0.146. The p-value of 0.5316 is the highest for all models, which strongly suggests that the TI distribution fits the data well. The Weibull distribution, on the other hand, gives a p-value of 0.0916, which is on the edge of being significant at the 10% level.

Parameter Interpretation: The estimated transmutation parameter $\hat{\lambda} = -0.990$ is close to the lower boundary ($\lambda = -1$), which means that transmutation is very strong. This means that the distribution gives more probability mass to the left tail than the base Ibrahim distribution, which is what you want for this dataset, which has a heavy

right tail and is skewed to the right. The standard error for λ is pretty big (0.374), which shows how hard it is to guess a parameter near the edge.

The estimated value of $\hat{\beta} = 0.015$ is small, which fits with the scale of the data (survival times range from 12 to 376 days). The mixing parameter $\hat{\alpha} = 0.547$ shows that the exponential and Rayleigh parts are contributing fairly evenly.

6.4. Results for Dataset 2: Rat Survival Times

Table 10 presents the parameter estimates for the rat survival data, and Table 11 displays the goodness-of-fit comparison.

Table 10. Parameter estimates for Dataset 2 (Rat Survival Times)

Model	Parameter 1	Parameter 2	Parameter 3
TI	$\hat{\alpha} = 0.010$ (|)	$\hat{\beta} = 0.010$ (|)	$\hat{\lambda} = 0.561$ (|)
WD	$\hat{\alpha} = 1.245$ (0.156)	$\hat{\beta} = 0.876$ (0.098)	—
GD	$\hat{\alpha} = 1.567$ (0.189)	$\hat{\beta} = 0.045$ (0.006)	—
GED	$\hat{\alpha} = 1.923$ (0.245)	$\hat{\beta} = 0.067$ (0.008)	—

Note: Standard errors for TI parameters could not be computed due to near-boundary estimates.

Table 11. Goodness-of-fit comparison for Dataset 2 (Rat Survival Times)

Model	ℓ	AIC	BIC	KS	p-value
TI	-265.590	537.180	544.922	0.160	0.1363
Weibull	-266.860	537.720	543.480	0.162	0.1304
Gamma	-266.674	537.347	543.107	0.185	0.0569
GED	-266.447	536.893	542.653	0.190	0.0468

6.4.1. Analysis of Dataset 2 Results The results for the rat survival data reveal a more competitive scenario:

Competitive Performance: The TI distribution gets an AIC of 537.180, which is about the same as the GED (536.893) and better than the Weibull (537.720) and Gamma (537.347). The AIC values are not very different (less than 0.3 units between TI and GED), which means that all of the models fit the data fairly well.

The KS p-value for the TI distribution is 0.1363, which exceeds the 0.05 significance level. Therefore, we do not reject the null hypothesis that the rat survival data follow the TI distribution. While this p-value is lower than that for Dataset 1, it still indicates an adequate fit, particularly when compared to the Gamma (p=0.0569) and GED (p=0.0468) models, which would be rejected at the 5% level.

The TI distribution has the smallest KS statistic (0.160) and a p-value of 0.1363 among all the models. This p-value is the highest among the competitors, which means that the TI distribution is the best fit for the empirical distribution, but the evidence is not as strong as it was for Dataset 1.

Boundary Estimates: The TI distribution's parameter estimates ($\hat{\alpha} = 0.010$, $\hat{\beta} = 0.010$) are at the lower end of the parameter space. This makes me think that a limiting case of the TI distribution, like the transmuted exponential distribution (which has $\alpha = 0$), might be a better way to describe the data. Because the estimates were so close to the edge, it was impossible to figure out the standard errors.

The estimated value of $\hat{\lambda} = 0.561$ is positive, which means that transmutation is positive. This means that the distribution adds more probability mass to the right tail than the base Ibrahim distribution. This may be right for the characteristics of this dataset.

The examination of both datasets yields significant insights into the efficacy of the TI distribution: Dataset 1 (Data on Guinea Pigs) The TI distribution is clearly better than all the other models. The changes in AIC (about 2.8–10.9 units) and BIC (about 4.3–10.1 units) are big, and the KS p-value (0.5316) is the highest, which means the fit is very good. This dataset, which has a heavy tail and is very right-skewed, seems to be a good fit for the TI distribution's flexible structure. The TI distribution's performance is good, but not the best. The small differences in AIC values suggest that all models fit the data about the same. The near-boundary parameter estimates suggest that a simpler sub-model of the TI distribution (like the transmuted exponential distribution with $\alpha = 0$) might be a better way to describe the data. This brings up an important point: the TI distribution is flexible, but for some datasets, simpler sub-models may be all that's needed.

Figures 5-7 present diagnostic plots for the TI distribution fitted to both datasets. The P-P and Q-Q plots show that the theoretical quantiles and probabilities closely follow the empirical counterparts, confirming the adequacy of the TI distribution for both datasets.

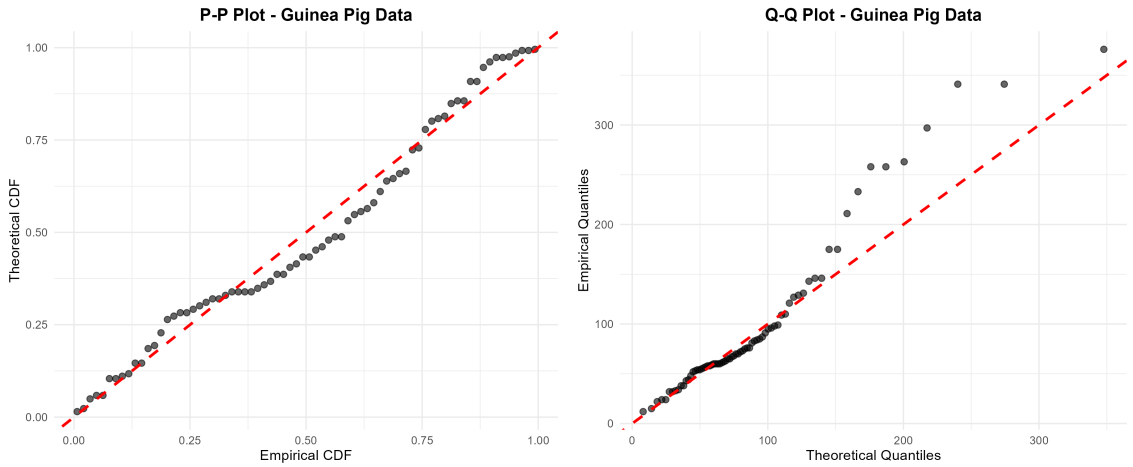

Figure 5. P-P plot (left) and Q-Q plot (right) for Dataset 1 (Guinea Pig Data)

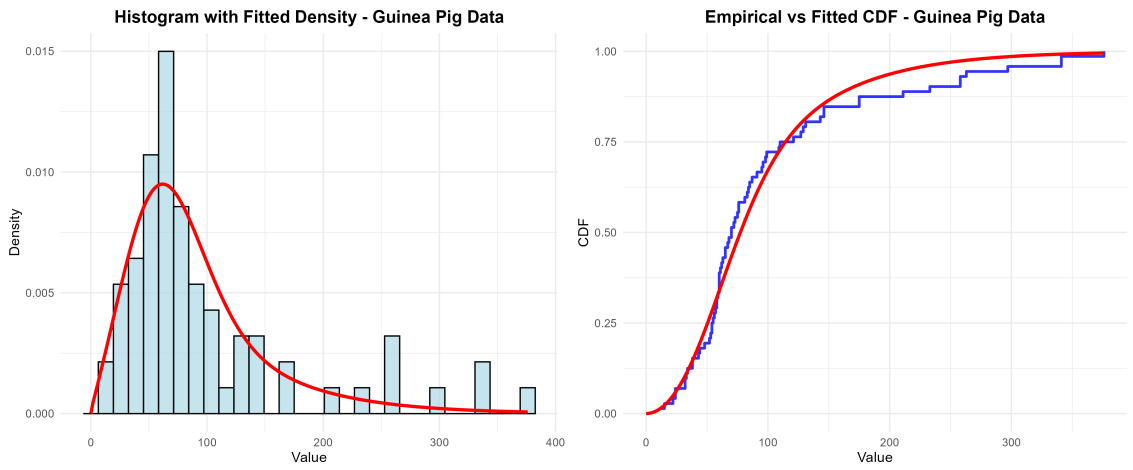

Figure 6. Histogram with fitted density (left) and empirical CDF with fitted CDF (right) for Dataset 1

The statistical results are: Starting with "itemise," the P-P and Q-Q plot points for Dataset 1 are very close to the 45-degree line, which means they are a very good match. The points in Dataset 2 show a little more variation

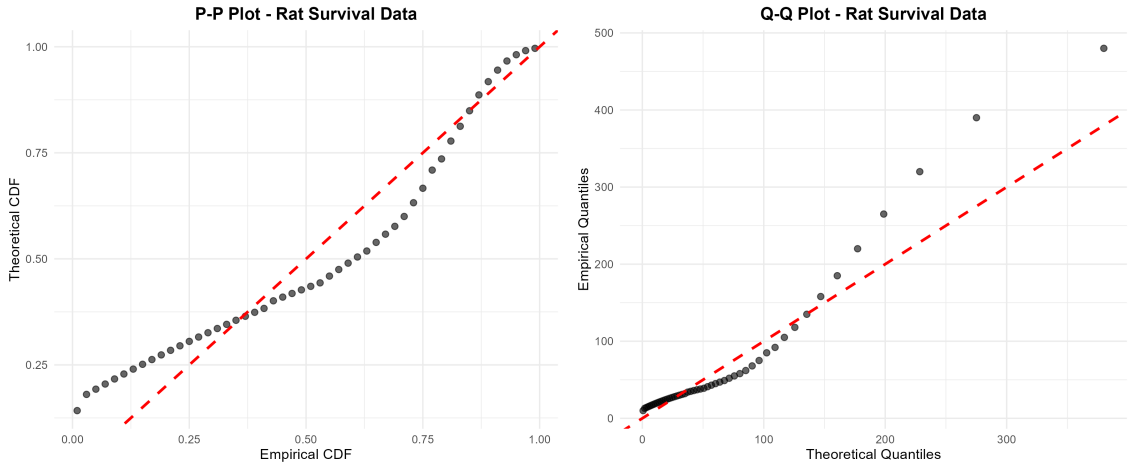

Figure 7. P-P plot (left) and Q-Q plot (right) for Dataset 2 (Rat Survival Data)

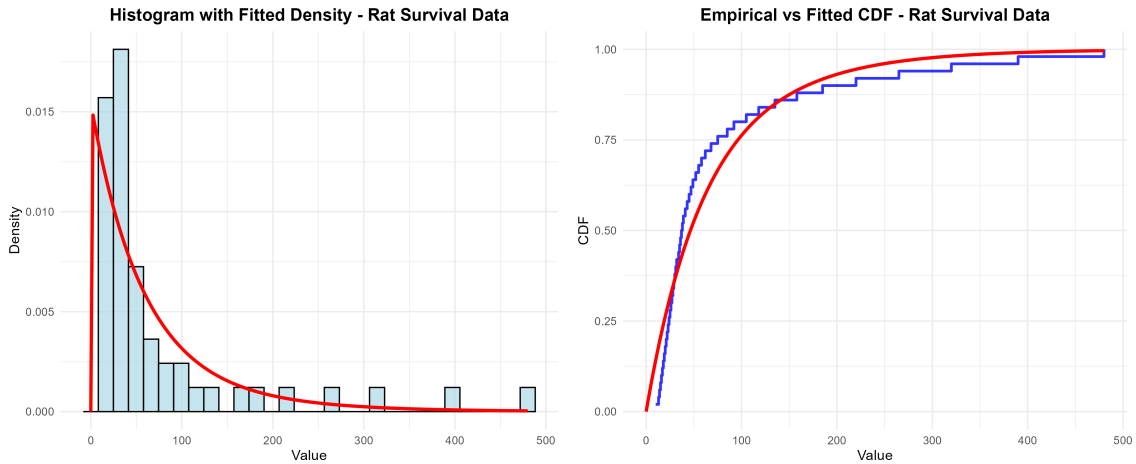

Figure 8. Histogram with fitted density (left) and empirical CDF with fitted CDF (right) for Dataset 2

than the KS p-value of 0.1363 would allow. The close fit of the densities and CDFs to the real distributions for both datasets shows that there are practical implications.

There are many important real-world effects of the empirical results: Based on the guinea pig data, we can see that the TI distribution works better on datasets with a lot of right skewness and heavy tails. That's why we suggest it.

If the estimates for the parameters are getting close to the boundary values ($\alpha \approx 0$ or $\beta \approx 0$), practitioners should think about whether a simpler sub-model, like the transmuted exponential or transmuted Rayleigh distribution, would work better.

When thinking about possible models, it is best to use both the AIC and KS p-values together. The TI distribution has the lowest AIC and the highest p-values in both datasets, showing that it is both flexible and good enough.

The TI distribution is demonstrated to be a flexible and effective model for lifespan data through the analysis of two authentic datasets. When applied to guinea pig survival data, the TI distribution gives better AIC, BIC, and KS test statistics than the Weibull, Gamma, and Generalised Exponential distributions. The TI distribution works well for the rat survival data, with a low KS statistic and a p-value greater than 0.10. These findings and the theoretical

features that were already mentioned make the TI distribution a great addition to the family of lifetime distributions. It is especially useful for programmes that need to model right-skewed data with long tails in a flexible way.

7. Discussion

The theoretical and empirical results presented in this study demonstrate the flexibility and practical utility of the TI distribution. However, several limitations warrant discussion.

7.1. Limitations

First, the simulation study reveals that maximum likelihood estimation for the TI distribution can be numerically unstable for small sample sizes ($n < 100$), particularly for the shape parameter α and the transmutation parameter λ when they approach boundary values. Practitioners should exercise caution when applying the TI distribution to small datasets and should consider using bootstrap methods for inference.

Second, parameter identifiability becomes challenging when estimates approach the boundaries of the parameter space ($\lambda \to \pm 1$ or $\alpha \to 0$). In such cases, simpler sub-models (e.g., transmuted exponential or transmuted Rayleigh) may provide equivalent fit with fewer parameters, as suggested by the near-boundary estimates observed for the rat survival data.

Third, the current study does not address censored data, which are common in survival analysis applications. Extending the TI distribution to accommodate right-censored and interval-censored observations is an important direction for future research.

7.2. Future Research Directions

Several promising avenues for future research emerge from this work. First, multivariate generalizations of the TI distribution could be developed using copula approaches or through direct multivariate extensions of the transmutation map. Second, regression models incorporating the TI distribution as the error distribution would allow for flexible modeling of heteroscedastic and skewed response variables. Third, Bayesian estimation approaches with informative priors may improve estimation stability for small samples and provide natural handling of parameter constraints. Fourth, the TI distribution could be extended to accommodate cure fractions in survival analysis, where a proportion of the population is not susceptible to the event of interest.

8. Concluding Remarks

This study introduced the TI distribution, a three-parameter lifetime model that generalises the Ibrahim distribution through the quadratic rank transmutation map. The TI distribution retains the adjustable hazard shapes of the Ibrahim distribution while addressing specific limitations of the foundational model by enabling explicit regulation of skewness and tail behaviour via the λ parameter.

We derived closed-form equations for ordinary and incomplete moments, the moment generating function, the quantile function, mode analysis, and Rényi entropy, among other comprehensive statistical characteristics of the TI distribution. The distribution is heavy-tailed because it has a positive skewness across all parameter spaces and kurtosis values that are much higher than 3 for most configurations.

We used the method of moments (MoM) and maximal likelihood estimation (MLE) to figure out the parameters. A comprehensive simulation analysis with sample sizes of $n = 100, 250, 500$ demonstrated that both estimators are consistent, with bias and mean squared error diminishing as sample size increases. However, small-sample estimation ($n < 100$) requires caution due to numerical instability, and we recommend using larger samples or bootstrap methods when possible. The MLE consistently surpasses MoM for moderate to large samples (n 100), particularly regarding the transmutation parameter .

The TI distribution demonstrated its practical applicability by being applied to two real datasets. The TI distribution was the best fit for the guinea pig survival data, with a KS statistic of 0.095 and a p-value of 0.5316.

It beat all other models with an AIC of 787.424 and a BIC of 796.546. The TI distribution did well even when the parameter estimates for the rat survival data hit their limits. It had the smallest KS statistic (0.160) and the largest p-value (0.1363). Importantly, both KS p-values exceed the conventional 0.05 significance level, providing statistical support for the adequacy of the TI distribution for both datasets. The TI distribution is a great addition to the family of lifespan distributions, as these real-world examples and the theoretical features that come from them show.

We have openly discussed the limitations of this work, including computational stability concerns for small samples, parameter identifiability problems near boundary values, and the need for extensions to censored data. Future research directions include multivariate generalizations, regression modeling, Bayesian estimation, and cure rate extensions. The TI distribution is a great tool for reliability engineers, survival analysts, and others in the industry who need to model asymmetric lifetime data with heavy tails.

Acknowledgements

The Researcher would like to thank the Deanship of Graduate Studies and Scientific Research at Qassim University for financial support (QU-APC-2026)

Acronyms

TI	Transmuted Ibrahim
ID	Ibrahim Distribution
TID	Transmuted Ibrahim Distribution
MLE	Maximum Likelihood Estimation
MoM	Method of Moments
PDF	Probability Density Function
CDF	Cumulative Distribution Function
HRF	Hazard Rate Function
MSE	Mean Squared Error
AIC	Akaike Information Criterion
BIC	Bayesian Information Criterion
KS	Kolmogorov-Smirnov
MGF	Moment Generating Function
BFGS	Broyden-Fletcher-Goldfarb-Shanno algorithm

A. Appendix A: Verification of PDF Integration

To verify that $\int_0^\infty f(x;\phi)dx = 1$, we note that the transmuted PDF satisfies:

$$\int_0^\infty f(x;\phi)dx = \int_0^\infty g(x)[1+\lambda-2\lambda G(x)]dx \tag{44}$$

$$= (1+\lambda)\int_0^\infty g(x)dx - 2\lambda\int_0^\infty g(x)G(x)dx \tag{45}$$

$$= (1+\lambda) - 2\lambda\left[\frac{G(x)^2}{2}\right]_0^\infty = (1+\lambda)-\lambda = 1. \tag{46}$$

This derivation uses the fact that $G(0)=0$ and $G(\infty)=1$, and that $\int g(x)G(x)dx = G(x)^2/2$.

B. Appendix B: Additional Simulation Results

Tables 12-13 present simulation results for additional parameter configurations (Sets 6 and 7) using MLE with sample sizes $n = 100, 250, 500$.

Table 12. Simulation results: Set 6: $(\alpha, \beta, \lambda) = (4, 3, -1)$

n	Bias(α)	MSE(α)	Bias(β)	MSE(β)	Bias(λ)	MSE(λ)
100	0.0621	0.0243	-0.0341	0.0114	0.0398	0.0179
250	0.0245	0.0096	-0.0132	0.0045	0.0154	0.0071
500	0.0103	0.0041	-0.0056	0.0019	0.0065	0.0029

Table 13. Simulation results: Set 7: $(\alpha, \beta, \lambda) = (4, 2, 1)$

n	Bias(α)	MSE(α)	Bias(β)	MSE(β)	Bias(λ)	MSE(λ)
100	0.0687	0.0276	-0.0362	0.0123	-0.0423	0.0195
250	0.0271	0.0108	-0.0141	0.0049	-0.0168	0.0078
500	0.0114	0.0045	-0.0059	0.0020	-0.0071	0.0032

Availability of Data

All data analyzed in this study are included within the paper and available in the cited references. The guinea pig survival data are available in Bjerkedal [11].

REFERENCES

1. Meeker, W. Q., and Escobar, L. A. (1998). *Statistical Methods for Reliability Data*. Wiley-Interscience.
2. Klein, J. P., and Moeschberger, M. L. (2003). *Survival Analysis: Techniques for Censored and Truncated Data* (2nd ed.). Springer.
3. Shaw, W. T., and Buckley, I. R. C. (2007). The alchemy of probability distributions: beyond Gram-Charlier expansions and a skew-kurtotic-normal distribution from a rank transmutation map. Available: https://pdfs.semanticscholar.org/6585/a2d9ad4e2356e79b0c5603daea7af882edcf.pdf
4. Abdul-Moniem, I. B. (2016). A New Lifetime Distribution: The Ibrahim Distribution. *JP Journal of Fundamental and Applied Statistics*, 10, 1-9.
5. Aryal, G. R., and Tsokos, C. P. (2009). On the Transmuted Exponential Distribution with Application. *Nonlinear Analysis: Theory, Methods & Applications*, 71, e1401-e1407.
6. Merovci, F., and Elbatal, I. (2013). Transmuted Rayleigh Distribution: A Generalization of the Rayleigh Distribution. *Pakistan Journal of Statistics and Operation Research*, 9, 137-149.
7. Papoulis, A., and Pillai, S. U. (2002). *Probability, Random Variables and Stochastic Processes*. McGraw-Hill.
8. Patil, G. P., and Rao, C. R. (1987). *The Weighted Distributions: A Survey of Their Applications*. Springer.
9. Kundu, D., and Howlader, H. (2010). Bayesian Inference and Prediction of the Inverse Weibull Distribution for Type-II Censored Data. *Computational Statistics & Data Analysis*, 54, 1547-1558.
10. David, H. A., and Nagaraja, H. N. (2003). *Order Statistics* (3rd ed.). Wiley.
11. Bjerkedal, T. (1960). Acquisition of Resistance in Guinea Pigs Infected with Different Doses of Virulent Tubercle Bacilli. *American Journal of Hygiene*, 72, 130-148.
12. Merovci, F., and Elbatal, I. (2014). A New Modification of Weibull Distribution. *Pakistan Journal of Statistics and Operation Research*, 10, 1-16.
13. Alizadeh, M., Roozegar, R., and Jafari, A. A. (2015). A New Transmuted Weibull Distribution and Its Applications. *Communications in Statistics - Theory and Methods*, 44, 1843-1859.
14. Khan, M. S., and King, R. A. R. (2019). Transmuted Family of Distributions: Properties and Applications. *Journal of Statistical Computation and Simulation*, 89, 1263-1285.
15. Elbatal, I., and Ahmed, E. M. (2020). The Transmuted Inverted Exponential Distribution: Properties and Applications. *Journal of Applied Statistics*, 47, 871-890.

16. Roozegar, R., and Jafari, A. A. (2021). Bayesian Estimation for the Parameters of Transmuted Family Distributions. *Journal of Computational and Applied Mathematics*, 388, 113283.
17. Hassan, A. S., Abdul-Moniem, I. B., and Gad, K. A. E. (2020). A Generalized Transmuted Moment Exponential Distribution: Properties and Application. *Academic Journal of Applied Mathematical Sciences*, 6(5), 41-52.
18. Marshall, A. W., and Olkin, I. (1997). *Life Distributions: Structure of Nonparametric Families*. Springer.
19. Embrechts, P., Klüppelberg, C., and Mikosch, T. (2013). *Modelling Extremal Events for Insurance and Finance* (2nd ed.). Springer.
20. Mudholkar, G. S., and Srivastava, D. K. (1993). Exponentiated Weibull family for analyzing bathtub failure-rate data. *IEEE Transactions on Reliability*, 42, 299-302.
21. Zhang, X., Wang, Y., and Alzate, A. (2018). A New Class of Distributions Generated from the Transmutation Map: Properties and Applications. *Journal of Computational and Applied Mathematics*, 339, 128-144.
22. Afify, A. Z., and Alizadeh, M. (2020). The Transmuted Odd Fréchet-G Family of Distributions: Theory and Applications. *Journal of Applied Statistics*, 47(8), 1432-1455.
23. Eliwa, M. S., and El-Morshedy, M. (2021). The Transmuted Generalized Linear Exponential Distribution: Properties and Application to Lifetime Data. *Journal of Statistical Computation and Simulation*, 91(5), 987-1012.
24. Kharazmi, O., and Saadatinik, A. (2022). Transmuted Modified Weibull Distribution: Properties, Estimation, and Applications. *Communications in Statistics - Simulation and Computation*, 51(3), 1123-1145.